

Article - Biological and Applied Sciences

Biosynthesis of Graphene and Investigation of Antibacterial Activity of Graphene-*parthenium hysterothorax* Nanocomposite

Naeem Akbar¹

<https://orcid.org/0000-0001-5436-0990>

Sidra Kanwal¹

<https://orcid.org/0000-0002-8931-6997>

Muhammad Shafiq Ahmed^{1*}

<https://orcid.org/0000-0002-9563-9741>

Simab Kanwal²

<https://orcid.org/0000-0003-4085-1232>

Muhammad Ashfaq Jamil¹

<https://orcid.org/0000-0003-0299-3926>

Sabastine Ezugwu³

<https://orcid.org/0000-0002-9755-6456>

Muhammad Saleem⁴

<https://orcid.org/0000-0002-3685-648X>

Said Nasir Khisro¹

<https://orcid.org/0000-0002-6280-7411>

Muhammad Javed¹

<https://orcid.org/0000-0002-1401-4943>

Nasar Ahmed⁵

<https://orcid.org/0000-0003-0460-6571>

Ahsan Ejaz⁶

<https://orcid.org/0000-0002-9679-6327>

¹University of Kotli Azad Jammu and Kashmir, Department of Physics, Kotli, AJK, Pakistan; ²Mahidol University, Institute of Molecular Biosciences, Salaya, Phuttamonthon, Nakhon Pathom, Thailand; ³University of Western Ontario, Department of Physics and Astronomy, London ON, Canada; ⁴University of Kotli Azad Jammu and Kashmir, Department of Chemistry, Kotli, AJK, Pakistan; ⁵Azad Jammu and Kashmir University, Department of Physics, Muzaffarabad, AJK, Pakistan; ⁶Mirpur University of Science and Technology, Department of Civil Engineering, Mirpur, AJK, Pakistan.

Editor-in-Chief: Alexandre Rasi Aoki
Associate Editor: Fábio André dos Santos

Received: 2021.03.26; Accepted: 2021.07.21.

*Correspondence: mshafiq@uokajk.edu.pk, Tel: +9233339463669 (M. S. A.).

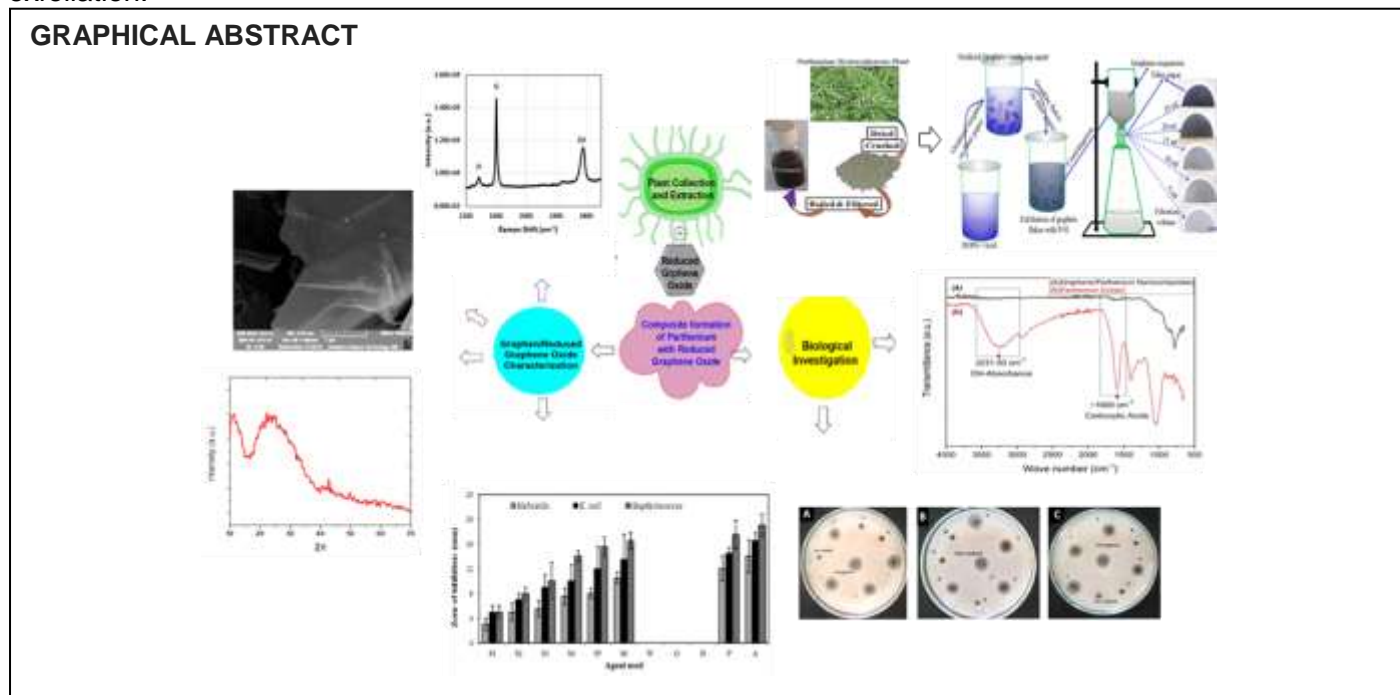
HIGHLIGHTS

- Biosynthesis of graphene using extract of *Parthenium hysterothorax* (P-H) as surfactant.
- Antibacterial activity of Graphene/*Parthenium hysterothorax* (G/P-H) was found to be controlled by graphene content in the G/P-H nanocomposite.
- Biocompatible graphene has a potential to be used in biomedical applications.

Abstract: There is a great interest to use carbon-based material like graphene and graphene oxide in biomedical applications due to its flexibility to be functionalized with bio-active molecules. Herein, graphene and graphene-based nanocomposites were biosynthesized by liquid-phase exfoliation of graphite using aqueous extract of *Parthenium hysterothorax* (P-H) as a surfactant. A set of five thin film samples of

graphene was prepared from graphene suspension by vacuum filtration method. Samples were characterized by UV-vis spectroscopy, Raman spectroscopy, SEM, and XRD, which revealed successful synthesis of graphene. Graphene/P-H(G/P-H) nanocomposites comprising varied ratios of graphene and P-H were prepared and their antibacterial activity was investigated by agar well diffusion method. The experimental results indicated that G/P-H nanocomposite have higher antibacterial activity than graphene alone, and bioactivity of G/P-H nanocomposite was found to be controlled by the fraction of graphene in the composite.

Keywords: Graphene; *Parthenium hysterophorus*; nanocomposite; biosynthesis; bioactivity; liquid-phase exfoliation.



INTRODUCTION

Graphene is a planar sheet of single layered atoms of carbon, possessing unusual properties such as tunable electronic band gap, double surface area, very high mechanical strength, ultra-high density and outstanding thermal conductivity [1-6]. This two-dimensional (2D) material has acquired enormous consideration because of its use in many electronic and optoelectronic devices like transparent electrode in solar cell, light emitting diodes, and touch screens [7-10]. Graphene and reduced graphene oxide have been used in biological and medical application like stem cell regeneration [11], DNA sequencing [12], dental and medical applications [13]. Nanocomposites of graphene have shown enhanced properties because of inclusion of graphene in them. Lot of work has already been reported previously on Graphene based nanocomposites, for example graphene-ZnO nanocomposites and graphene-Cu nanocomposites are used for batteries and supercapacitor applications [3,14-16]. In biomedical applications graphene-based composites were also used. A small concentration of few layer graphene (0.2 %) used to fabricate dental-polymer composites showed improved physio-mechanical properties [17]. Reduced graphene oxide nanomaterials have been used in scaffolds' structure to enhance bone regeneration and also displayed antimicrobial activity [18]. Graphene quantum dots were used in photolytic therapy [19].

Graphene is generally produced by chemical vapor deposition (CVD) [20], chemical reduction of graphene oxide or thermal treatment of graphene oxide [21-23] and mechanical exfoliation of graphite with sonication in the presence of solvent or chemical /biological surfactant [24-27]. A simple, green method for the synthesis of RGO/Ag nanocomposite using the amino acid tyrosine as bioreductant and stabilizing agent has been reported already by S.B. Sireesh Babu Maddinedi and coauthors [28]. Various biological techniques for synthesis of graphene using extracts of plant are reported in literature. These techniques, for synthesis of graphene, are used due to their high-yield, nontoxicity, low cost and environmentally benign procedures adopted [29, 30]. Spinach leaf and *Xanthium strumarium* extracts have been used to prepare reduced graphene oxide and few layered graphene [30, 31].

In this work, *Parthenium heterosporous* extract (P-H) is used as an organic surfactant for stabilization of exfoliated graphene flakes. Also, graphene/P-H (G/P-H) nanocomposite was made and its antibacterial

activity was investigated against different bacterial strains. To the best of our knowledge the use of P-H for synthesis of graphene is not reported yet. *P. hysterophorus* is a noxious, herbaceous and exotic weed belonging to asteraceae family. It grows in agricultural lands, orchards, forest lands and food plains [32, 33]. However, this plant has many useful chlorogenic acids, such as caffeic acid, p-coumaric acid, ferulic acid, vanillic acid and p-anisic acid, that are beneficial for bio-medical and industrial use. [33]. *P. hysterophorus* based graphene nanocomposite can be used in many applications where biocompatibility of graphene is important.

MATERIAL AND METHODS

The chemicals and other materials used in this work include highly oriented pyrolytic graphite (HOPG), sulphuric acid, nitric acid, acetone, ethanol, and nitrocellulose filters. Analytical grade chemicals have been purchased from Sigma-Aldrich, while filter papers with a pore size of 220 nm have been purchased from Millipore.

Preparation of *Parthenium hysterophorus* extract

The selected plant *P. hysterophorus* was collected from Mandi Dhara, Kotli District, Azad Jammu and Kashmir State, Pakistan. Fresh aerial parts of plant material, i.e. stem and leaves, were collected, washed and dried in open air for 9 days. The total weight of the plant used to prepare the extract was 191.4 g. The dried plant material was crushed into pieces and two distinct methods of extraction were followed. The stem and leaves weighing 35 g were extensively washed with distilled water for three times and dipped into the glass beaker containing 200 ml of distilled water. The mixture was boiled at 80 °C for one hour and cooled to room temperature followed by filtration to negate the dust particles using Whatman-42 filter paper. The filtrate was then permitted to stand for ten days at room temperature to evaporate the remaining solvents. The second method was to macerate the crushed stem and the 5 g leaves into the distilled water in 200 ml of distilled water, so that the water content was higher than that of the plant. The mixture was boiled for up to two hours at 100 °C and cooled to room temperature, followed by filtration with whatman42 filtering paper. Figure 1 shows a stepwise process of preparation of leaves and stems extract of *P. hysterophorus*.

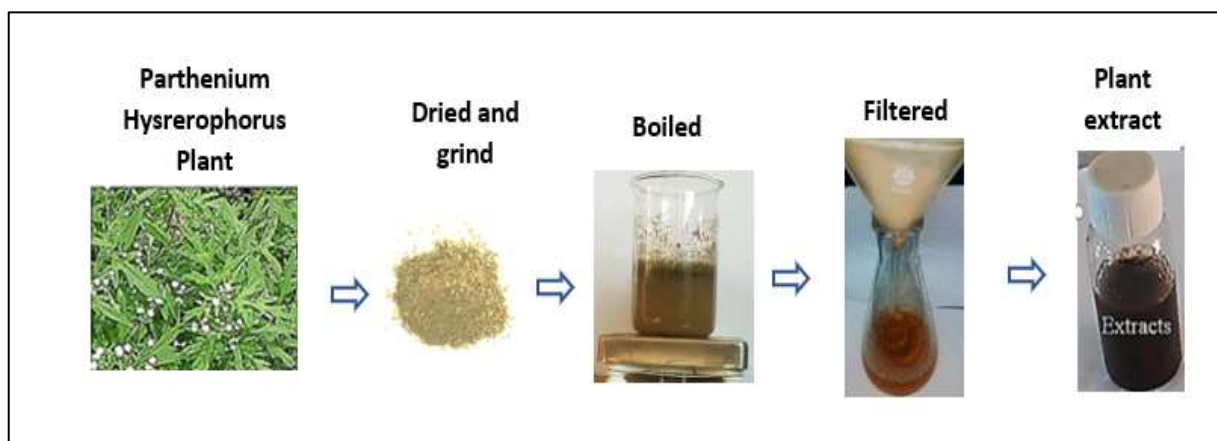


Figure 1. Preparation of an aqueous extract of *P. hysterophorus*. The starting materials are the stems and leaves of *P. hysterophorus*, which are then air dried for 9 days. Dried *P. hysterophorus* leaves and stems are easy to crush to powdery state, allowing the complete extraction upon boiling at 80 °C.

Synthesis of graphene thin films and graphene/*Parthenium hysterophorus* nanocomposite

To synthesize the graphene thin films, HOPG powder was chemically treated with a H₂SO₄:HNO₃ (3:1) mixture for 12 h, which resulted in a mildly oxidized graphite suspension. As shown in Figure 2, the oxidized graphite was first collected on Millipore filter membrane (pore size 220 nm), followed by dispersion and sonication in the reducing agent. The resulting graphite flakes on the filter membrane were washed with deionized water several times, dried, and subsequently used for the preparation of graphene suspensions.

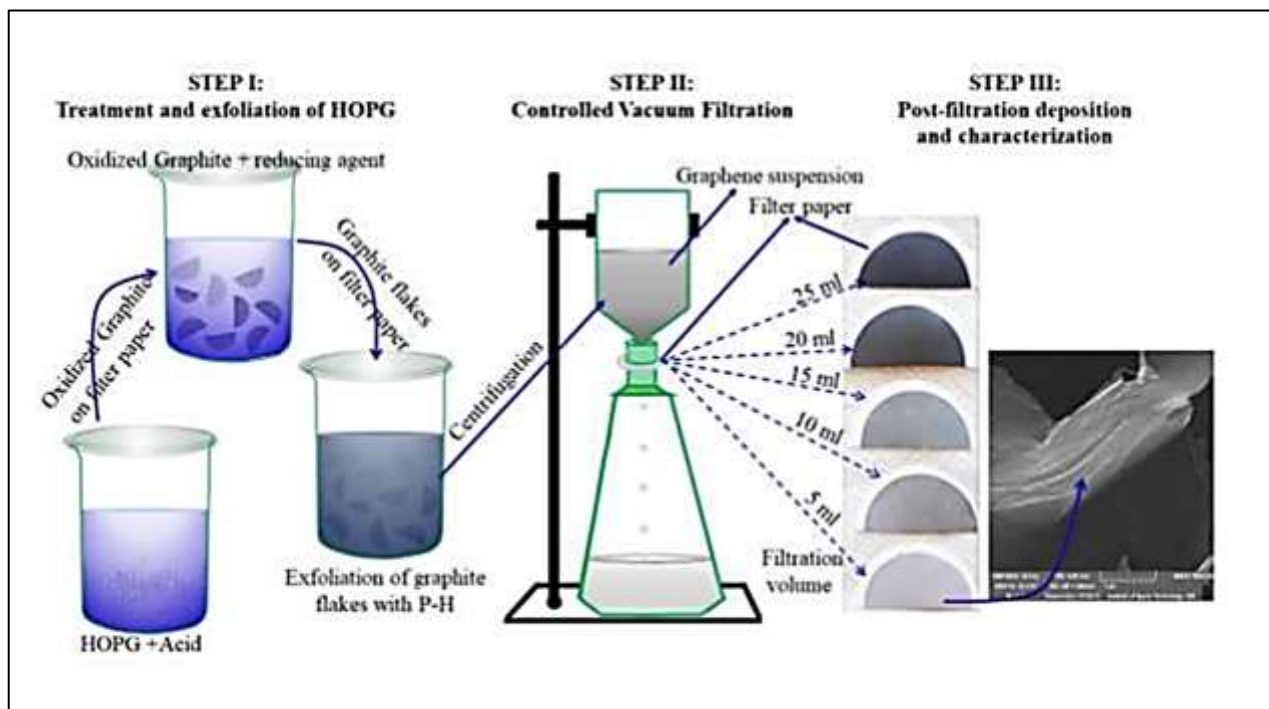


Figure 2. Schematic demonstration of steps of graphene thin films and graphene/*P. hysterophorus* (G/P-H) nanocomposites. STEP I: Chemical treatment of Highly Oriented Pyrolytic Graphite (HOPG). STEP II: Suspension of few-layer graphene and G/P-H nanocomposites used to prepare samples by vacuum filtration. STEP III: The SEM image of a large flake of G/P-H nanocomposite made from 5 mL filtration volume of the suspension.

A modified Hummer's procedure was adopted to synthesize the G/P-H nanocomposite using the P-H as an organic surfactant to exfoliate and stabilize few layer graphene. Graphene suspension was prepared by dispersing treated graphite in P-H. Briefly, treated graphite (0.8 g) was added to 500 mL of the solution and sonicated it for 5 h. The suspension was left overnight on a stable surface to allow the formation of thick, non-exfoliated graphite sediments. The upper 50% of this suspension was decanted and centrifuged (at 6000 rpm) for 30 min. The supernatant fraction was collected and subjected to vacuum filtration to generate the graphene flakes on nitrocellulose filter membranes (MCE, Millipore) (STEP II, Figure 2). Five thin film samples were prepared in this way from different filtration volumes of graphene suspensions, from 5 mL to 25 mL (STEP III, Figure 2).

The thin film of graphene was transferred to glass substrates by placing the filter paper with graphene flakes on the substrate under load and dried. Filter papers were etched by successive acetone and methanol baths, leaving behind graphene thin films on substrates. The same suspension of graphene was used to prepare G/P-H nano-mixture by mixing the graphene suspension with P-H in varying ratios of graphene and P-H suspensions in water. Six samples of G/P-H nanocomposite were prepared by changing the ratios of graphene and P-H suspensions as given below:

Graphene suspension/*Parthenium* composite: S1- 0.1 mL/10 mL, S2 - 0.1 mL /12 mL, S3 - 0.1 mL /14 mL, S4 - 0.1 mL /16 mL, S5 - 0.1 mL /18 mL and S6 - 0.1 mL /20 mL. Sample S1 has higher concentration of graphene in the nanocomposite as compared to Sample S6.

Characterization

Morphological study was done by taking SEM micrographs taken with MIR TESCAN SEM at different magnifications. Raman spectrum of a typical graphene base thin film was taken by (DV420-OE). The optical analysis of the prepared samples was performed using UV-visible spectroscopy within the wavelength range from 400 to 900 nm. The optical transmittance measurement was carried out at room temperature using the (Data Stream-CE3000) spectrophotometer series.

Antibacterial assay

Antibacterial activity of G/P-H against non-pathogenic bacteria (*Escherichia coli*) and pathogenic bacterial strains (*Staphylococcus aureus* and *Klebsiella pneumonia*) was assessed by using a modified agar well diffusion method [34]. Briefly, 1 mL of overnight grown bacterial cultures were pipetted in LB nutrient

agar in a glass flask and mixed well at room temperature. The mixed LB nutrient agar and inoculum was poured into sterile glass petri dishes and wells were made using a 6 mm diameter sterile cork borer upon solidification of agar plates containing inoculums. Then 100 μL of each test sample were introduced to the respective wells nanocomposites of different concentrations) and plates were incubated at 37°C for 24 hours in culture media. A measure of the area of inhibition around the wells after the incubation period was described as antibacterial activity. Graphene (alone) in water and P-H dissolved in 5mg/mL of dimethyl sulfoxide (DMSO) were also tested for their antibacterial activity. Distilled water and DMSO were used as negative controls, whereas ampicillin (100 $\mu\text{g}/\text{mL}$) was used as a reference drug.

RESULTS

Scanning electron microscopy of graphene based thin films

Graphene based thin films samples with different film thickness were characterized by scanning electron microscope (SEM) for morphological study. SEM micrographs of the samples are shown in Figure 3.

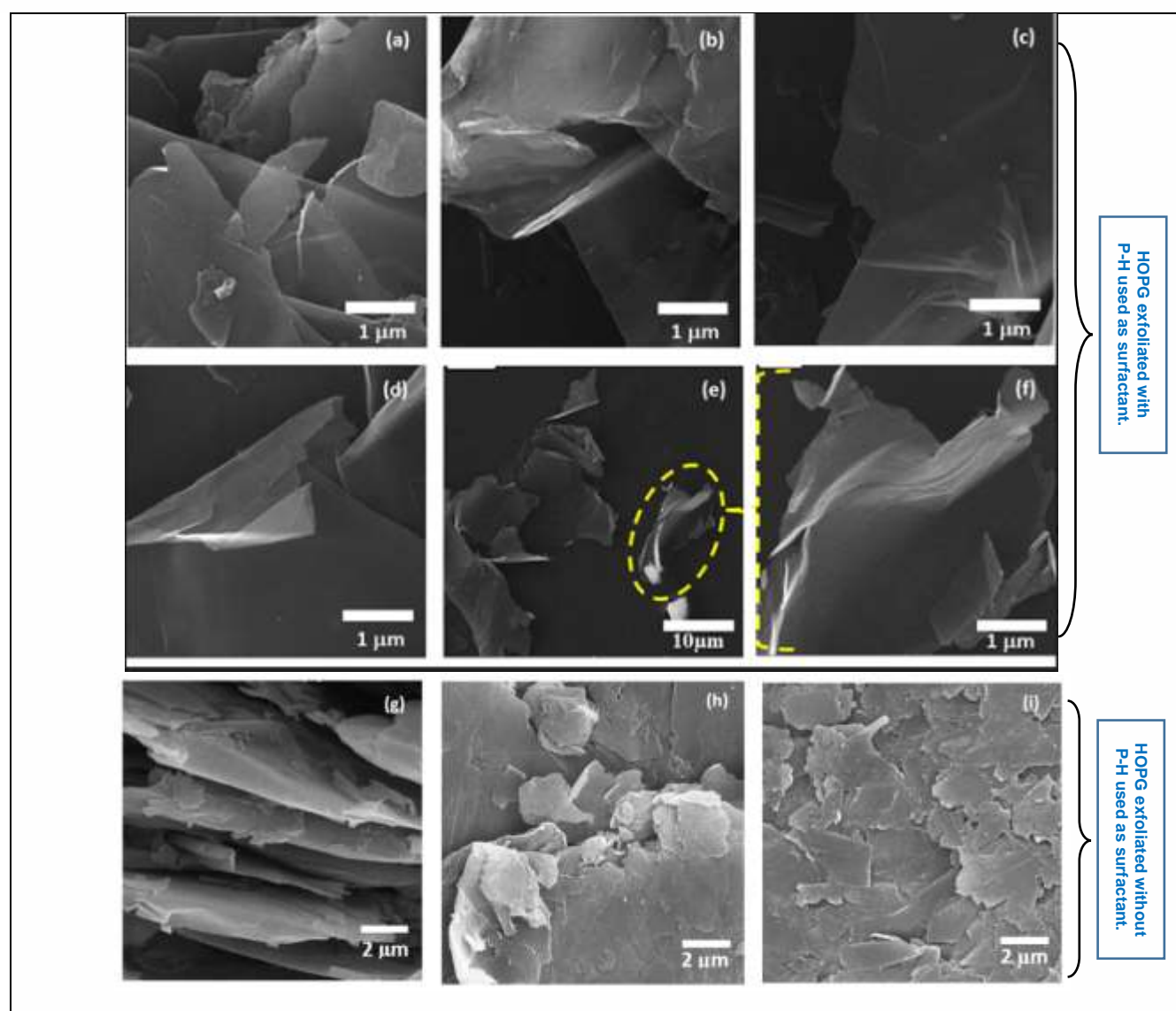


Figure 3. SEM images of graphene flakes exfoliated with P-H as surfactant from different filtration volumes of (a) 25 mL, (b) 20mL, (c) 15 mL, (d) 10 mL (e) 5 mL at low magnification and (f) 5 mL at higher magnification and (g-i) 15 mL sample without surfactant, showing graphitic thin films.

All SEM images are taken at same magnification except the sample prepared from 5 mL that includes a micrograph at low magnification to show the dispersion of graphene flakes on the substrate. From the SEM micrographs, graphene flakes can be seen clearly, indicating that the HOPG exfoliated into multi-layers graphene flakes of different sizes. The samples presented in panels (g-i) were prepared in the same condition

as the previous samples (panels a-f) but without the P-H surfactant. The SEM images of these samples show clearly that the HOPG did not exfoliate but retained as graphite films. The use of our biosynthesized P-H surfactant is a necessary condition to effectively exfoliate the HOPG to obtain multilayers graphene flakes as shown above.

Fourier Transform Infrared Spectroscopy analysis

The P-H extract and G/P-H nanocomposite were analyzed by FTIR to identify the functional groups of the extract that are possibly responsible for the capping of graphene. FTIR spectra of both P-H extract and G/P-H are shown in Figure 4.

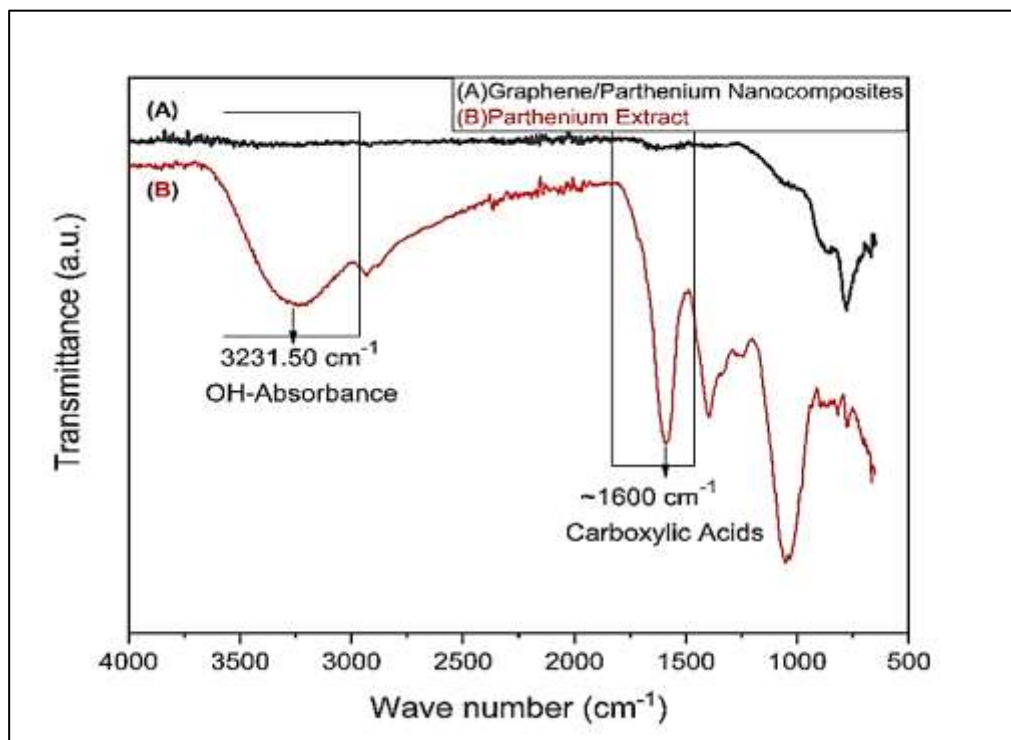


Figure 4. FTIR spectra of both P-H extract and G/P-H

The FT-IR spectrum of the P-H extract, depicted peaks at 3500 to 3100, 1725, 1415 cm^{-1} and 1000 cm^{-1} which represent the OH functional group in molecule and OH involving hydrogen bonds, carbonyl group (C-O) and stretching C-C aromatic ring vibrations, respectively. Polyphenolics and other chemicals within P-H extract act as surfactant and prevent agglomeration of graphene.

Raman analysis

Graphene based thin films were further characterized by Raman Spectroscopy to confirm the existence of graphene. Figure 5 shows the Raman spectrum of a typical sample, obtained by filtering very small (5 mL) amount of suspension of graphene. Three peaks: D, G and 2D at 1350 cm^{-1} , 1580 cm^{-1} and 2700 cm^{-1} respectively, can be clearly seen.

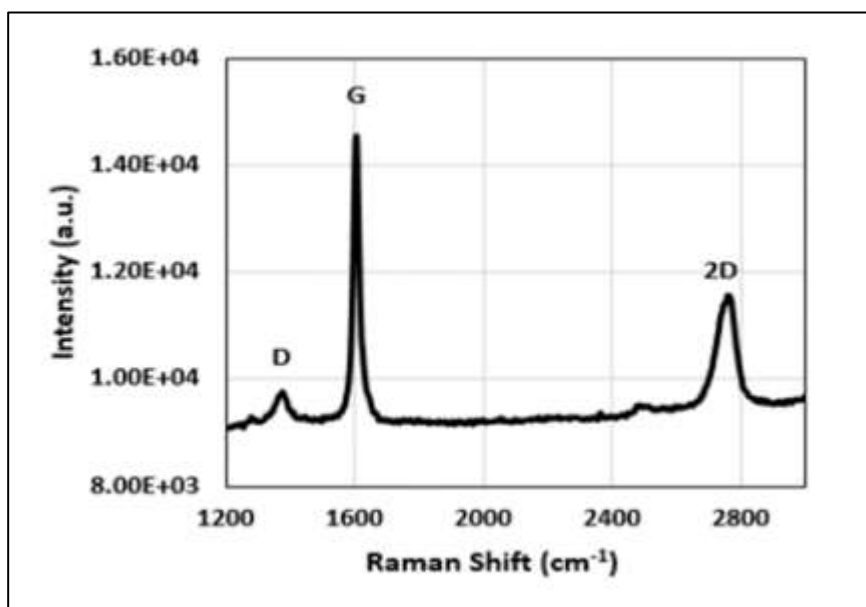


Figure 5. Raman spectrum of graphene based thin film sample.

The D peak is related with imperfection formed, in the graphene flakes in the samples, during deposition process while the G peak is attributed to sp^2 domains. The second-order Raman D mode (2D) is the signature of few- or multilayer graphene. In multilayer graphene, the intensity of the G peak is expected to be greater than the 2D peak and at the same time, the D and G peak intensity ratio (I_D/I_G) describes the density of disorder in the graphene [35]. This ratio is found to be 0.75 for the film deposited from 20 ml filtration volume of the graphene suspension, which suggests that the defects ratio is low and the quality of our graphene is good. The ratio of the intensities of 2D and G bands gives the concept of number of layers in graphene flake. For a single layer of relatively “ideal” graphene, reported value of $(I_{2D}/I_G) > 1$ [35]. In the case of multilayer graphene the ratio (I_{2D}/I_G) is found to decrease. Other authors reported low (I_{2D}/I_G) for solution-processed, single-layer graphene flakes [36].

X-Ray diffraction (XRD) analysis

The XRD spectrum of the thinnest graphene based thin film from the set of films prepared in this work is measured in the range of 2θ from 10° to 70° as shown in Figure 6.

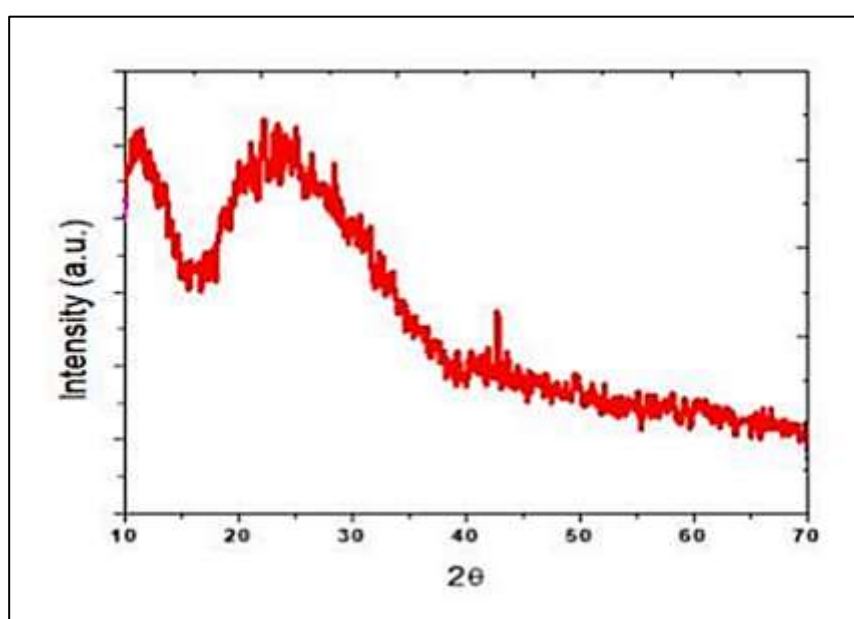


Figure 6. XRD pattern of a typical sample of graphene thin films.

The XRD profile exhibits a broad peak centered at $2\theta=23.4^\circ$ and is indexed as (002) diffraction plane corresponding to hexagonal crystal structure of graphene and another peak at $2\theta=42.7^\circ$ indicates that there is short range order of stacked graphene layers. The XRD spectrum of graphene sample shows a peak at $2\theta=10.9^\circ$ which corresponds to an interplanar spacing of 0.8 nm. The interplanar distance increased due to presence of functional groups [37]. The XRD pattern of the sample shown in Figure 6 is in conformity with the standard x-ray diffractograms of graphene samples prepared using well-known chemical surfactants such as SDBS [38]. This shows the effectiveness of the biosynthesized P-H extract to exfoliate graphite materials and concurrently acts to stabilize the graphene from re-aggregation.

Optical Characterization of thin films

Optical study of prepared thin film samples prepared with different filtration volumes of graphene suspension, was conducted by UV-visible spectroscopy with the wavelength range of 400 nm to 900 nm using Data Stream (CE3000 series) spectrophotometer. It is clear from the UV-vis spectra as shown in Figure 7, that all the samples have very low absorption in the visible region of spectrum, because graphene transparent in visible region of the spectrum and optical absorption increases with increasing number of layers. Optical absorption peak at 272 nm is characteristic of graphene. For our graphene based thin films samples the optical absorption increases with increasing filtration volume as the thickness of films increases with increasing filtration volume due to overlapping graphene flakes.

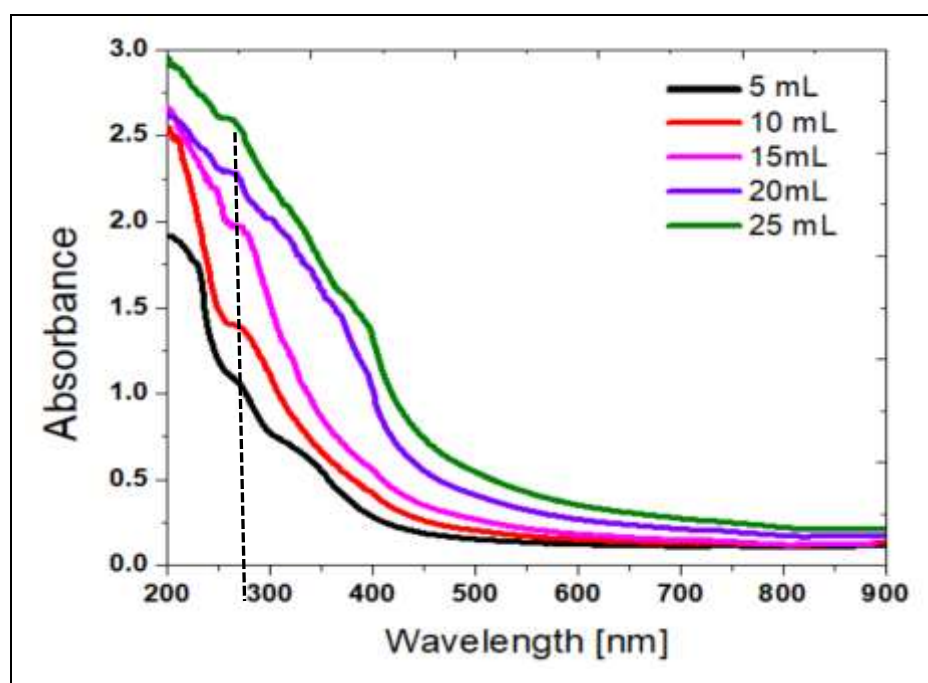


Figure 7. UV-Vis spectra of set of graphene based thin film samples prepared from different filtration volumes.

Evaluation of antibacterial activity of graphene/P. hysterothorax nanocomposite

Antibacterial activity of G/P-H nanocomposite samples (S1 to S6) having various ratios of graphene and P-H, with highest concentration of graphene in S1 and least in S6, was investigated by agar well diffusion method against *E. coli*, *S. aureus* and *K. pneumonia*. The Gram-negative bacterium *E. coli* is the naturally occurring human gut bacteria and commonly used microbe in the laboratories as a model organism owing to its non-pathogenic nature. Whereas Gram-positive and Gram-negative bacteria *S. aureus* and *K. pneumonia* respectively, are the pathogenic strains well known to cause various skin and lung infections in human. G/P-H nanocomposite showed varied levels of inhibition against selected bacterial strains as summarized in Table 1.

Table 1. Zones of inhibitions (mm) against various bacterial strains.

Bacterial strains	S1	S2	S3	S4	S5	S6	W	G	D	P	A
<i>K. pneumonia</i>	3.0	5.0	5.5	7.5	8.0	10.5	0.0	0.0	0.0	12.0	14.0
<i>E. coli</i>	5.0	7.0	9.0	10.0	12.0	13.5	0.0	0.0	0.0	14.5	16.5
<i>S. aureus</i>	5.0	8.0	10.0	14.0	15.5	16.5	0.0	0.0	0.0	17.5	19.0

G/P-H nanocomposite samples (S₁, S₂, S₃, S₄, S₅, S₆), Water (W), Graphite alone (G), DMSO (D), *P. hysterothorus* (P), Ampicillin (A).

The antibacterial activity of graphite alone (G) and aqueous extract of P-H (P) was also monitored during this study. Distilled water (W) and DMSO (D) were used as negative controls in antibacterial tests and they were found to have no inhibitory effect on bacterial growth. Ampicillin was used as a reference drug (positive control). It was noticed that with increasing concentration of P-H in the graphene-based suspension, the inhibitory effect of G/P-H nanocomposite against all tested bacterial strains was increased, with maximum inhibition caused by S₆ against *S. aureus* (Figure 8). P-H also showed antibacterial activity with the inhibition zones of 14.5 mm, 17.5 mm and 12 mm against *E. coli*, *S. aureus* and *K. pneumonia*, respectively as shown in Figure 8.

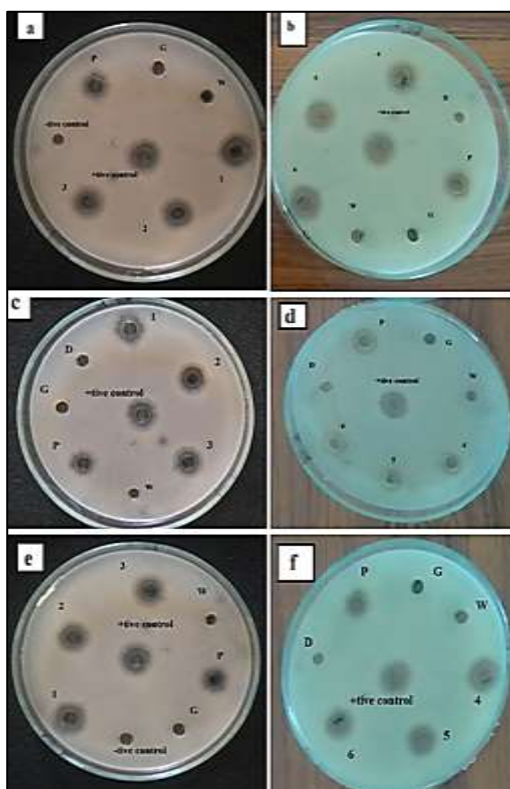


Figure 8. The effect of G/P-H nanocomposites against *K. pneumonia* (a,b), *E. coli* (c,d) and *S. aureus* (e,f). G/P-H nanocomposite samples, water (W), Aqueous extract of *P. hysterothorus* (P), graphite alone (G), ampicillin (+tive control), DMSO (D).

DISCUSSION

Scanning electron microscopy images demonstrate that thin films samples contain graphene flakes that were stabilized in the suspension with the help of P-H extract. The P-H contains a large number of functional groups with both a hydrophobic base and hydrophilic sites as shown in Figure 9 (Schematic of attachment of functional groups of P-H with graphene layers).

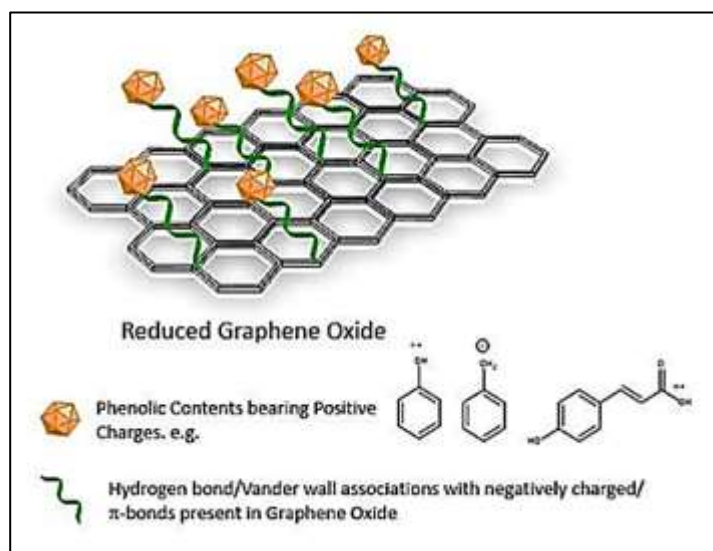


Figure 9. Schematic of attachment of functional groups of P-H extract with graphene layer via Vander walls bonding.

The attachment of such groups to the graphene layers prevents/limits the aggregation of graphene in water and creates the conditions for steric stabilization of graphene sheets, by preventing them from re-approaching once they have been intercalated. The functional group of P-H, with hydrophobic bases adhere to the graphene lattice via van der Waals forces and keep graphene suspended in water. It can be seen in Figure 4 that the prominent peaks of carbonyl groups and broad spectrum of OH is reduced (almost vanished), which gives an indication of maximum interaction of carbonyl groups with graphene surface bound groups. Raman spectrum of our sample has the ratio of intensities of 2D and G bands (I_{2D}/I_G) equal to 0.85, which means that the graphene flakes in our samples are likely to have large concentrations of impurities as generally is the case with the solution processed films. From XRD result, the absence of sharp peak at $2\theta=26^\circ$ in XRD profile of our sample is a clear indication of absence of graphite showing that HOPG was successfully exfoliated into few layers graphene with the help of P-H extract as surfactant.

Antibacterial activity of G/P-H nanocomposite samples showed that the inhibitory effect of the nanocomposite, against all tested bacterial strains, increased with increasing concentration of Parthenium extract in the nanocomposite. The maximum inhibition was caused by S6 against *S. aureus* (Figure 8). It was reported previously that aqueous extract of *P. hysterophorus* leaves has high antibacterial potency owing to the presence of bioactive compounds [37]. Whereas no antibacterial activity of graphite alone was observed against any of the tested bacterial strains (as shown in Figure 10), showing that graphite did not interrupt the action of P-H and might be acting as a delivery agent rendering P-H as the main active component.

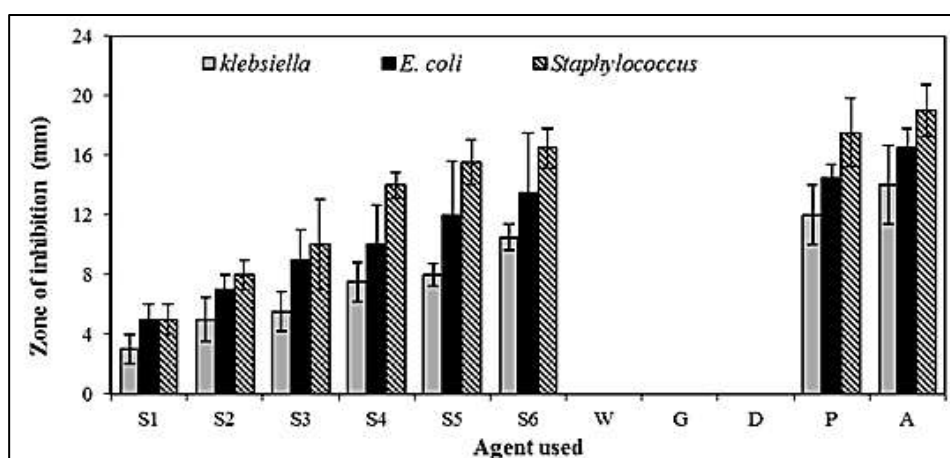


Figure 10. Antibacterial activity of various G/P-H samples (S1-S6), Graphite alone (G) and *P. hysterophorus* (P), against *K. pneumoniae*, *E. coli*, and *S. aureus*. Water (W) and DMSO (D) were used as negative controls, and 100 $\mu\text{g}/\text{mL}$ Ampicillin (A) was used as reference drug.

The results indicated that *S. aureus* was highly susceptible to P-H and G/P-H nanocomposite as compared to *E. coli* and *K. pneumonia* which showed comparatively less susceptibility. Apart from prokaryotic bacterial cells, graphene is also known for having cytotoxic effect on eukaryotic cells owing to its physicochemical characteristics and interactions with cell organelles. The cytotoxicity of graphene is mostly induced by *in vivo* DNA damage and change of gene expression leading to lose in cell functionality and cell death [39, 40]. It is worth mentioning that graphene does not support bacterial growth as well as it does not hinder normal bacterial growth, as evident from Figure 10 that graphene (G) did not have any zone of inhibition. However, P-H alone had shown higher zone of inhibition than all of the composite samples (S1 to S6) with different concentrations of graphene. It is observed that nanocomposite samples (such as S1 and S2) having higher quantity of graphene and less quantity of P-H in the nanocomposite showed rather less antibacterial activity because of lower concentration of P-H (Figure 8) owing to possible chemical interactions among compounds in P-H extract and graphene. Further studies regarding the biological activities of G/P-H nanocomposites and chemical interactions among graphite and P-H in G/P-H nanocomposite shall provide insights into the detailed underlying mechanisms of G/P-H nanocomposite properties.

CONCLUSION

Few layers graphene was successfully obtained through the modified hummer's method with the use of new type of surfactant. *P. hysterophorus* extract was used as a surfactant for successful exfoliation of treated graphite and preparation of graphene suspension. A new biocompatible and eco-friendly non-ionic surfactant is introduced in this work to be used for synthesis of graphene. Thin film samples prepared from the graphene suspension were investigated for morphology, structure and vibrational modes by employing SEM, XRD and Raman spectroscopy which confirmed the successful formation of graphene and exfoliation of graphite. SEM micrographs showed graphene flakes of different sizes, indicating that the HOPG exfoliation occurred in the presence of P-H extract. XRD pattern showed a broad peak at $2\theta = 23.4^\circ$ corresponding to hexagonal crystal structure of graphene and another peak at $2\theta = 42.7^\circ$ indicates that there is short range order of stacked graphene layers. The XRD spectrum of graphene sample showed a peak at $2\theta = 10.9^\circ$ which is indication of increased inter-planar spacing (0.8 nm) indication restacking of graphene layers during filtration process. Raman spectra showed that the synthesized graphene has relatively less defects. Also, UV-vis spectra showed characteristic optical transmittance with very little absorption in the visible range. Such biocompatible graphene can be used in biosensors, other devices and applications where the biocompatibility of graphene films is required. In addition, bioactivity of G/P-H nanocomposite against different bacterial strains showed that concentration of graphene in the composite can be tuned to control the bioactivity of P-H as graphene alone did not show inhibition against bacterial growth, but G/P-H nanocomposite with different ratios of graphene and P-H showed varied levels of inhibition. It was found that higher concentration of graphene in the composite limited the bioactivity of P-H, which can be further investigated to tailor the properties of P-H based bioactive substances for medical applications.

Funding: Financial support is provided by Higher Education Commission (HEC) of Pakistan through project Nos. NRP-10181/2019 and ISULL 1017/2017.

Acknowledgments: The authors are thankful to the Biotechnology Laboratory, University of Kotli AJK for providing the technical support. Technical support of Mr. Yasir Iqbal from Mirpur University of Technology, for XRD, Mr. Muhammad Amjad from COMSATS Islamabad for SEM work and Mr. Sarfraz Ahmed from AJK University Muzaffarabad for Raman Spectroscopy and Mr. Ali Subhani, University of Kotli AJK for support in Bioactivity investigations, are highly acknowledged.

Conflicts of Interest: The authors declare that they have no known competing financial interests or personal relationships that could have appeared to influence the work reported in this paper.

REFERENCES

1. Geim AK. Graphene: status and prospects. *Science*. 2009;324(5934):1530-4.
2. Geim AK, Novoselov KS. The rise of graphene. *Nanoscience and technology: a collection of reviews from nature journals*: World Scientific; 2010. p. 11-9.
3. Goli P, Ning H, Li X, Lu CY, Novoselov KS, Balandin AA. Thermal properties of graphene-copper-graphene heterogeneous films. *Nano letters*. 2014;14(3):1497-503.
4. Nika D, Pokatilov E, Askerov A, Balandin A. Phonon thermal conduction in graphene: Role of Umklapp and edge roughness scattering. *Physical Review B*. 2009;79(15):155413.
5. Singh V, Joung D, Zhai L, Das S, Khondaker SI, Seal S. Graphene based materials: past, present and future. *Progress in materials science*. 2011;56(8):1178-271.

6. Nika D, Ghosh S, Pokatilov E, Balandin A. Lattice thermal conductivity of graphene flakes: Comparison with bulk graphite. *Appl. Phys. Lett.* 2009;94(20):203103.
7. Kumar N, Pruthi V. Structural elucidation and molecular docking of ferulic acid from *Parthenium hysterophorus* possessing COX-2 inhibition activity. *3 Biotech.* 2015;5(4):541-51.
8. Wang X, Zhi L, Müllen K. Transparent, conductive graphene electrodes for dye-sensitized solar cells. *Nano letters.* 2008;8(1):323-7.
9. Zhai T, Wang F, Yu M, Xie S, Liang C, Li C, et al. 3D MnO₂-graphene composites with large areal capacitance for high-performance asymmetric supercapacitors. *Nanoscale.* 2013;5(15):6790-6.
10. Zhang Y, Li H, Pan L, Lu T, Sun Z. Capacitive behavior of graphene-ZnO composite film for supercapacitors. *J. Electroanal. Chem.* 2009;634(1):68-71.
11. Hu S, Zeng Y, Yang S, Qin H, Cai H, Wang J. Application of Graphene Based Nanotechnology in Stem Cells Research. *J. Nanosci. Nanotechnol.* 2015;15(9):6327-41.
12. Heerema SJ, Dekker C. Graphene nanodevices for DNA sequencing. *Nature Nanotechnology.* 2016;11(2):127-36.
13. Han Xie TC, Francisco Javier Rodríguez-Lozano, Emma Kim Luong-Van, Vinicius Rosa. Graphene for the development of the next-generation of biocomposites for dental and medical applications. *Dental Materials.* 2017;33(7):765-74.
14. Mitra S, Lokesh K, Sampath S. Exfoliated graphite-ruthenium oxide composite electrodes for electrochemical supercapacitors. *J. Power Sources.* 2008;185(2):1544-9.
15. Peng L, Feng Y, Lv P, Lei D, Shen Y, Li Y, et al. Transparent, conductive, and flexible multiwalled carbon nanotube/graphene hybrid electrodes with two three-dimensional microstructures. *The J. Phys. Chem C.* 2012;116(8):4970-8.
16. Chang T, Li Z, Yun G, Jia Y, Yang H. Enhanced photocatalytic activity of ZnO/CuO nanocomposites synthesized by hydrothermal method. *Nano-Micro Letters.* 2013;5(3):163-8.
17. Malik S, Ruddock FM, Dowling AH, Byrne K, Schmitt W, Khalakhan I, et al. Graphene composites with dental and biomedical applicability. *Beilstein J. Nanotechnol.* 2018;9:801-8.
18. Cabral CSD, Miguel SP, de Melo-Diogo D, Louro RO, Correia IJ. Green reduced graphene oxide functionalized 3D printed scaffolds for bone tissue regeneration. *Carbon.* 2019;146:513-23.
19. Sung S-Y, Su Y-L, Cheng W, Hu P-F, Chiang C-S, Chen W-T, et al. Graphene Quantum Dots-Mediated Theranostic Penetrative Delivery of Drug and Photolytics in Deep Tumors by Targeted Biomimetic Nanosponges. *Nano Lett.* 2019;19(1):69-81.
20. Yan Z, Peng Z, Sun Z, Yao J, Zhu Y, Liu Z, et al. Growth of Bilayer Graphene on Insulating Substrates. *ACS Nano.* 2011;5(10):8187-92.
21. Park S, Ruoff RS. Chemical methods for the production of graphenes. *Nature Nanotechnology.* 2009;4(4):217-24.
22. Tung VC, Allen MJ, Yang Y, Kaner RB. High-throughput solution processing of large-scale graphene. *Nature Nanotechnology.* 2009;4(1):25-9.
23. Zhou X, Liu Z. A scalable, solution-phase processing route to graphene oxide and graphene ultralarge sheets. *ChemComm.* 2010;46(15):2611-3.
24. Gravagnuolo AM, Morales-Narváez E, Longobardi S, da Silva ET, Giardina P, Merkoçi A. In Situ Production of Biofunctionalized Few-Layer Defect-Free Microsheets of Graphene. *Adv.Funct.Mater.* 2015;25(18):2771-9.
25. Hernandez Y, Nicolosi V, Lotya M, Blighe FM, Sun Z, De S, et al. High-yield production of graphene by liquid-phase exfoliation of graphite. *Nat. Nanotechnol.* 2008;3(9):563-8.
26. Lotya M, King PJ, Khan U, De S, Coleman JN. High-Concentration, Surfactant-Stabilized Graphene Dispersions. *ACS Nano.* 2010;4(6):3155-62.
27. Shin H-J, Kim KK, Benayad A, Yoon S-M, Park HK, Jung I-S, et al. Efficient Reduction of Graphite Oxide by Sodium Borohydride and Its Effect on Electrical Conductance. *Adv.Funct.Mater.* 2009;19(12):1987-92.
28. Sireesh Babu Maddinedi BKM, Nawaz Khan Fazlur-Rahman. High reduction of 4-nitrophenol using reduced graphene oxide/Ag synthesized with tyrosine. *Environ Chem Lett.* 2017.
29. Chabot V, Kim B, Sloper B, Tzoganakis C, Yu A. High yield production and purification of few layer graphene by Gum Arabic assisted physical sonication. *Scientific Reports.* 2013;3(1):1378.
30. Salunke BK, Kim BS. Facile synthesis of graphene using a biological method. *RSC Advances.* 2016;6(21):17158-62.
31. Gurunathan S, Kim J. H. Synthesis, toxicity, biocompatibility, and biomedical applications of graphene and graphene-related materials. *Int J Nanomedicine.* 2016;11:1927-45.
32. Meena RK, Dutt B, Kumar R, Sharma KR. Phyto-Chemistry of Congress grass (*Parthenium hysterophorus* L.) and Harmful and Beneficial effect on Human and Animals: A review. *IJCS.* 2017;5(4):643-7.
33. Kaur M, Aggarwal NK, Kumar V, Dhiman R. Effects and management of *Parthenium hysterophorus*: A weed of global significance. *International scholarly research notices.* 2014;2014.
34. Bauer AW, Kirby WM, Sherris JC, Turk M Antibiotic susceptibility testing by a standardized single disk method. *Am J Clin Pathol.* 1966;45:493-6.
35. Ferrari AC, Scardaci V, Casiraghi C, Lazzeri M, Mauri F, Piscanec S, et al. Raman Spectrum of Graphene and Graphene Layers. *Phys Rev Lett.* 2006; 97.
36. Casiraghi C. Doping dependence of the Raman peaks intensity of graphene close to the Dirac point. *Phys. Rev. B.* 2009;80(23):233407.

37. Sreejesh M, Nagaraja HS. Solar Exfoliated Graphene and its Application in Supercapacitors and Electrochemical H₂O₂ Sensing. *Electrochim. Acta* 160 (2015) 94–9.
38. Haixin Chang GW, An Yang, Xiaoming Tao, Xuqing Liu, Youde Shen and Zijian Zheng. A Transparent, Flexible, Low-Temperature, and Solution Processible Graphene Composite Electrode. *Adv. Funct. Mater.* 2010;20:10.
39. Zhou X, Vogt J, Spemann D, Yu W, Mao Z, Estrela-Lopis I, Donath E, Gao C. A quantitative study of the intracellular concentration of graphene/noble metal nanoparticle composites and their cytotoxicity. *Nanoscale* 2014;6:8535-42.
40. Gurunathan S, Park JH, Kim E, Choi YJ, Kwon DN, Kim JH. Reduced graphene oxide–silver nanoparticle nanocomposite: a potential anticancer nano therapy. *Int. J. Nanomed. Nanosurg.* 2015;10 6257-76.



© 2021 by the authors. Submitted for possible open access publication under the terms and conditions of the Creative Commons Attribution (CC BY NC) license (<https://creativecommons.org/licenses/by-nc/4.0/>).